nature portfolio

https://doi.org/10.1038/s41586-026-11035-z

Supplementary information

Evolution and heterogeneity of lethal metastatic bladder cancer subtypes

In the format provided by the authors and unedited

SUPPLEMENTARY INFORMATION

Evolution and heterogeneity of lethal metastatic bladder cancer subtypes

Pushpa Itagi[1,2]*, Samantha L. Schuster[1,2]*, Sonali Arora[2], Thomas W. Persse[1], Jennifer A. Waters[2], Michael Yang[1], Alan Min[1], Pooja Chandra[1], Mohamed Adil[1,2], Patricia C. Galipeau[1,2], Dmytro Rudoy[2], Allie S. Kreitman[3], Yixin Lin[2], Minjeong Ko[1], Erolcan Sayar[2], Robert D. Patton[1,2], Lori Kollath[4], Abby Meis[4], Samuel Lindergren[4], Nathan Ji[4], Khursheed Ali[4], Hrishi Venkatesh[5], Cynthia L. Wladyka[2], A. Patrick McDeed[1,2], Claire B. Mills[2,6], Manasvita Vashisth[1,2], Jin Yeong Kim[2], Rosa Nadal[7,8], Jessica Hawley[7,8], Todd Yezefski[7], Sarah P. Psutka[4], John L. Gore[4], Daniel W. Lin[1,4], Peter S. Nelson[1,2,3,4,8], Heather H. Cheng[7,8], Michael T. Schweizer[7,8], Lawrence Fong[5], John K. Lee[2,9], Evan Yu[7,8], Eva Corey[4], Colm Morrissey[4], Petros Grivas[7,8], Robert B. Montgomery[7], Jonathan L. Wright[4], Michael C. Haffner[2,8,10], Funda Vakar-Lopez[10], Omar Y. Mian[2,11,12]†, Hung-Ming Lam[4]†, Andrew C. Hsieh[2,3,7]†, Gavin Ha[1,2,3]†

[1] Public Health Sciences Division, Fred Hutchinson Cancer Center, 1100 Fairview Ave. N, Seattle, WA
[2] Human Biology Division, Fred Hutchinson Cancer Center, 1100 Fairview Ave. N, Seattle, WA
[3] Department of Genome Sciences, University of Washington, 1959 Pacific St, Seattle, WA
[4] Department of Urology, University of Washington, 1959 NE Pacific St, Seattle, WA
[5] Immunotherapy Integrated Research Center, Fred Hutchinson Cancer Center, 1100 Fairview Ave. N, Seattle, WA
[6] Department of Oral Health Sciences, University of Washington, 1959 NE Pacific St, Seattle, WA
[7] Division of Hematology & Oncology, Department of Medicine, University of Washington, 825 Eastlake Ave E, Seattle, WA
[8] Clinical Research Division, Fred Hutchinson Cancer Center, 1100 Fairview Ave. N, Seattle, WA
[9] Division of Hematology/Oncology, Department of Medicine and Institute of Urologic Oncology, Department of Urology, David Geffen School of Medicine at UCLA, 10833 Le Conte Avenue, Los Angeles, CA
[10] Department of Laboratory Medicine and Pathology, University of Washington, 1959 NE Pacific St, Seattle, WA
[11] Radiation Oncology Division, Fred Hutchinson Cancer Center, 1100 Fairview Ave. N, Seattle, WA
[12] Department of Radiation Oncology, University of Washington and Radiation Oncology Division, Fred Hutch Cancer Center, 1100 Fairview Ave. N, Seattle, WA
* Equal contribution
† Jointly supervised this work

Correspondence:

Gavin Ha, Ph.D.
Fred Hutchinson Cancer Center
1100 Fairview Ave. N,
Seattle, WA 98109
206-667-2802
gha@fredhutch.org

Andrew C. Hsieh, M.D.
Fred Hutchinson Cancer Center
1100 Fairview Ave. N,
Seattle, WA 98109
206-667-5871
ahsieh@fredhutch.org

Hung-Ming Lam, Ph.D.
University of Washington
1959 NE Pacific St.,
Seattle, WA 98195
206-543-1461
minglam@uw.edu

Omar Y. Mian, M.D, Ph.D.
Fred Hutchinson Cancer Center
1100 Fairview Ave. N,
Seattle, WA 98109
206-667-2802
omian@fredhutch.org

Supplementary Information

a

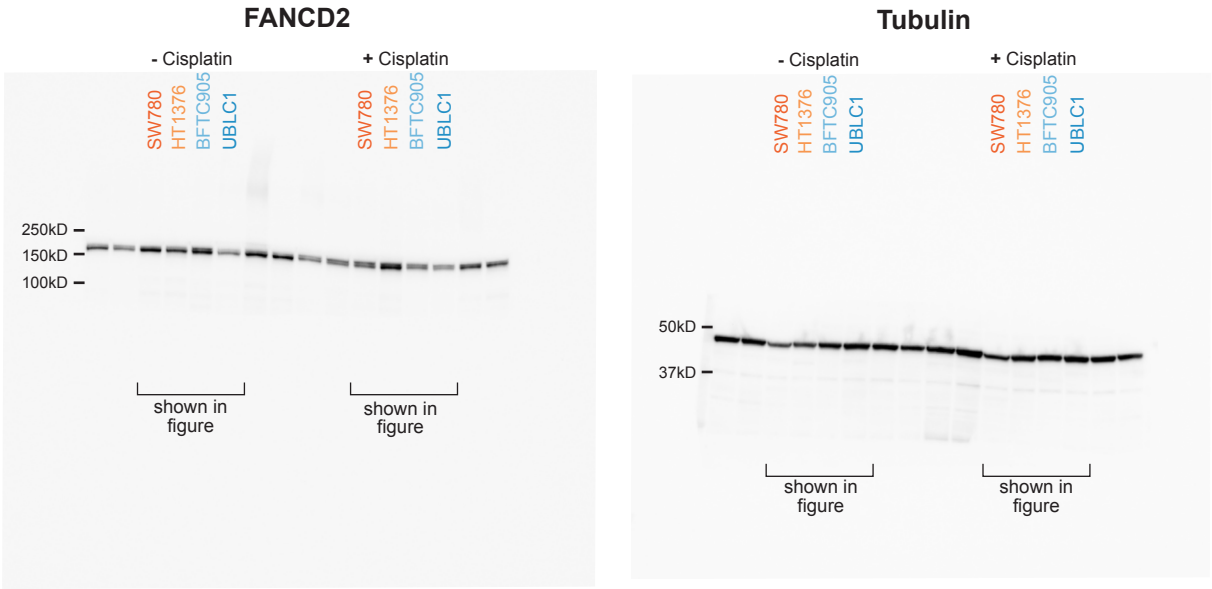
FANCD2
- Cisplatin
+ Cisplatin
SW780
HT1376
BFTC905
UBLC1
250kD
150kD
100kD
shown in figure
Tubulin
50kD
37kD

b

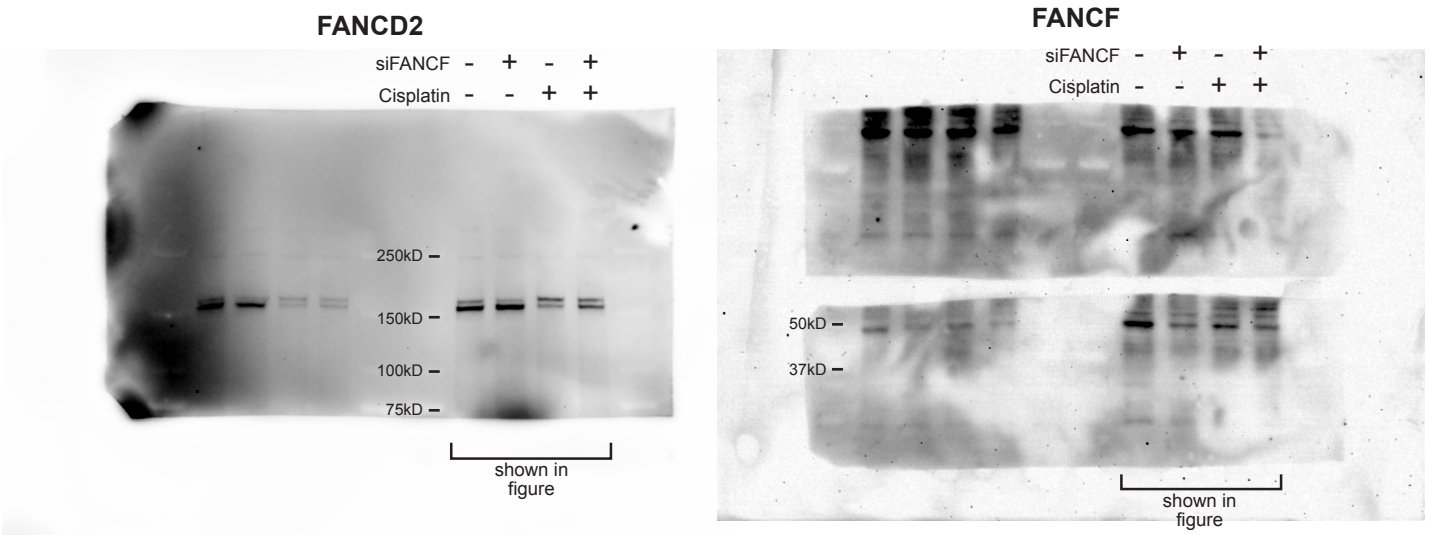
FANCD2
siFANCF - + - +
Cisplatin - - + +
250kD
150kD
100kD
75kD
shown in figure
FANCF
50kD
37kD

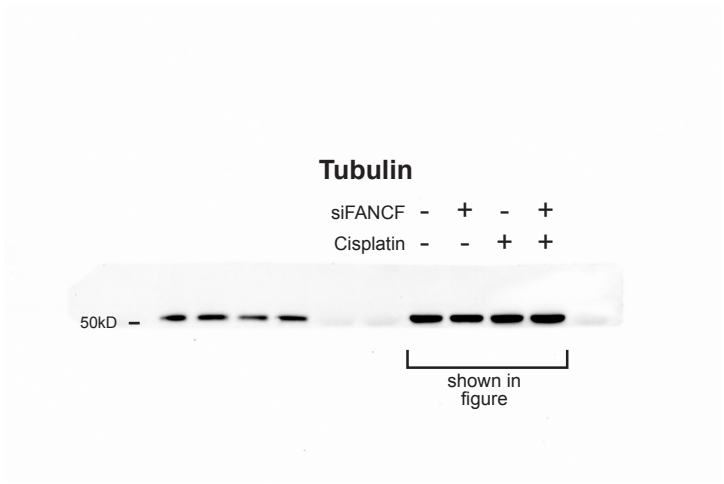
Tubulin
siFANCF - + - +
Cisplatin - - + +
50kD
shown in figure

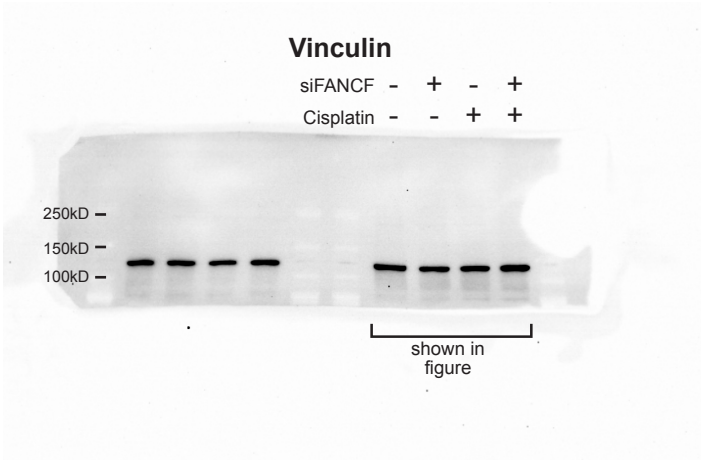
Vinculin
siFANCF - + - +
Cisplatin - - + +
250kD
150kD
100kD
shown in figure

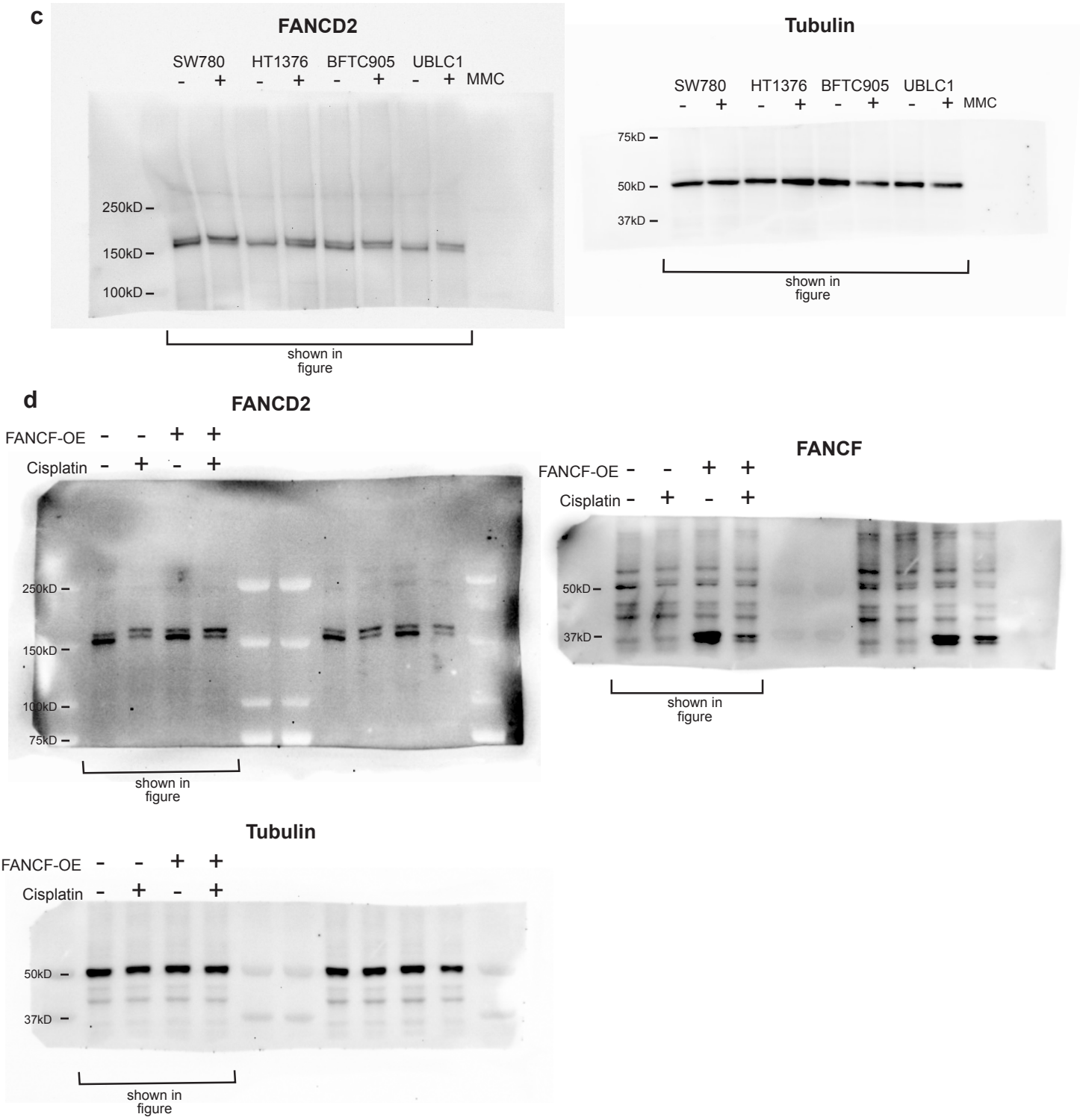

Supplementary Figure 1

a) Source gel images for **Figure 3f**. Black brackets indicate samples used for figure, with other samples not used for this analysis. Tubulin was run on the same gel and stained separately from FANCD2 as a loading control.

b) Source gel images for **Figure 3j**. Black brackets indicate sample set used for figure, with samples to the left representing another biological replicate. Tubulin and vinculin were used as loading controls for FANCD2 and FANCF, respectively. Each loading control was run on the same gel as the FANC protein and stained separately.

c) Source gel images for **Extended Data Fig. 6o**. All samples on this blot used in figure. Tubulin was run on the same gel and stained separately from FANCD2 as a loading control.

d) Source gel images for **Extended Data Fig. 7g**. Black brackets indicate samples used for figure, with samples to the right representing another biological replicate. Tubulin was used as a loading control for both FANCD2 and FANCF; blot was first probed for FANCD2 and FANCF, then stripped and the same blot probed for tubulin.

a

17-030: 14 month CT scan

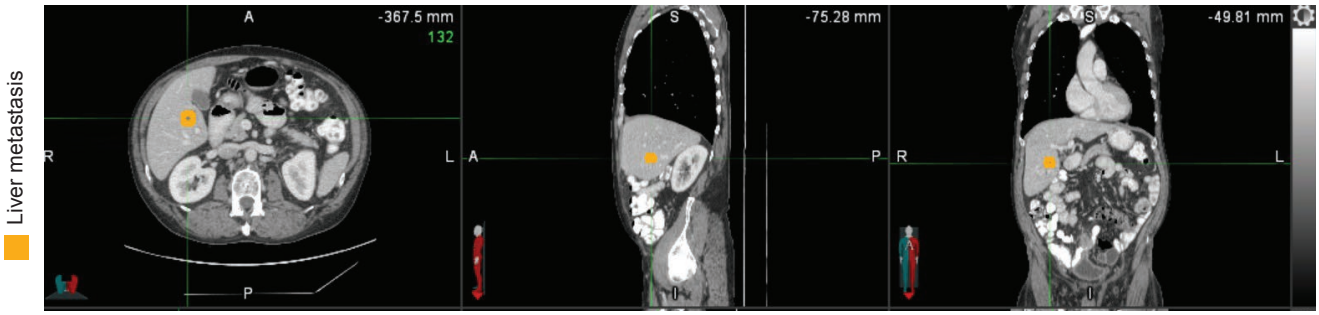

17-030: 17 month CT scan

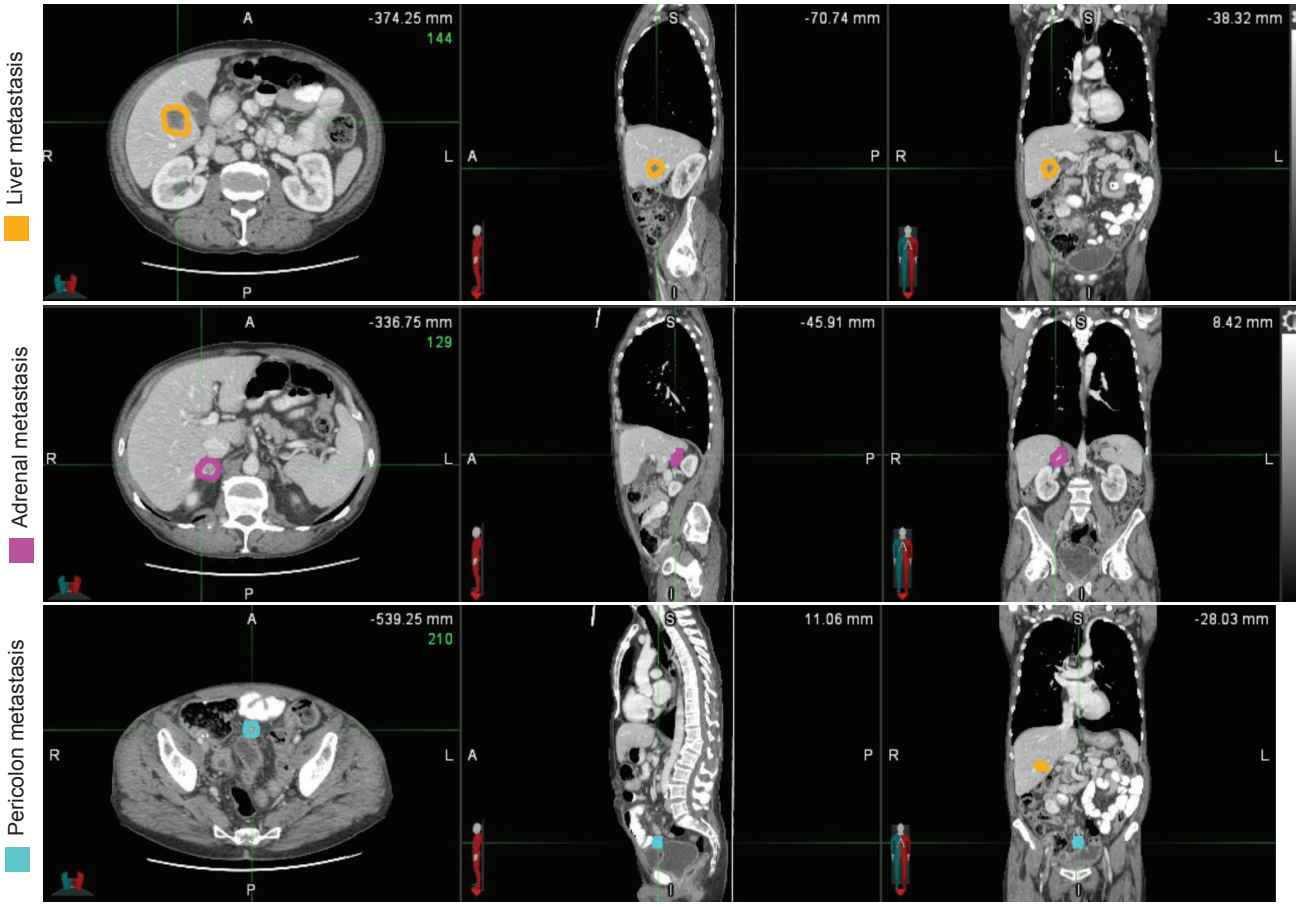

b

19-004: 47 month CT scan

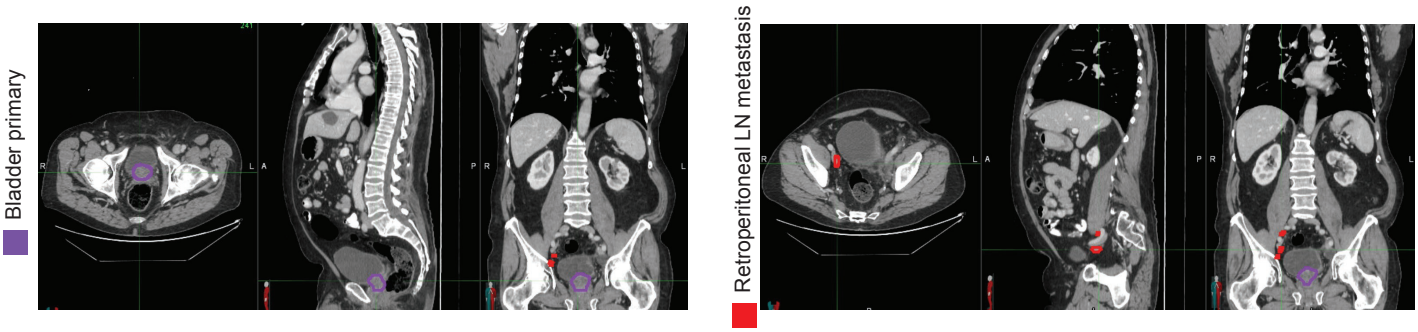

19-004: 54 month CT scan

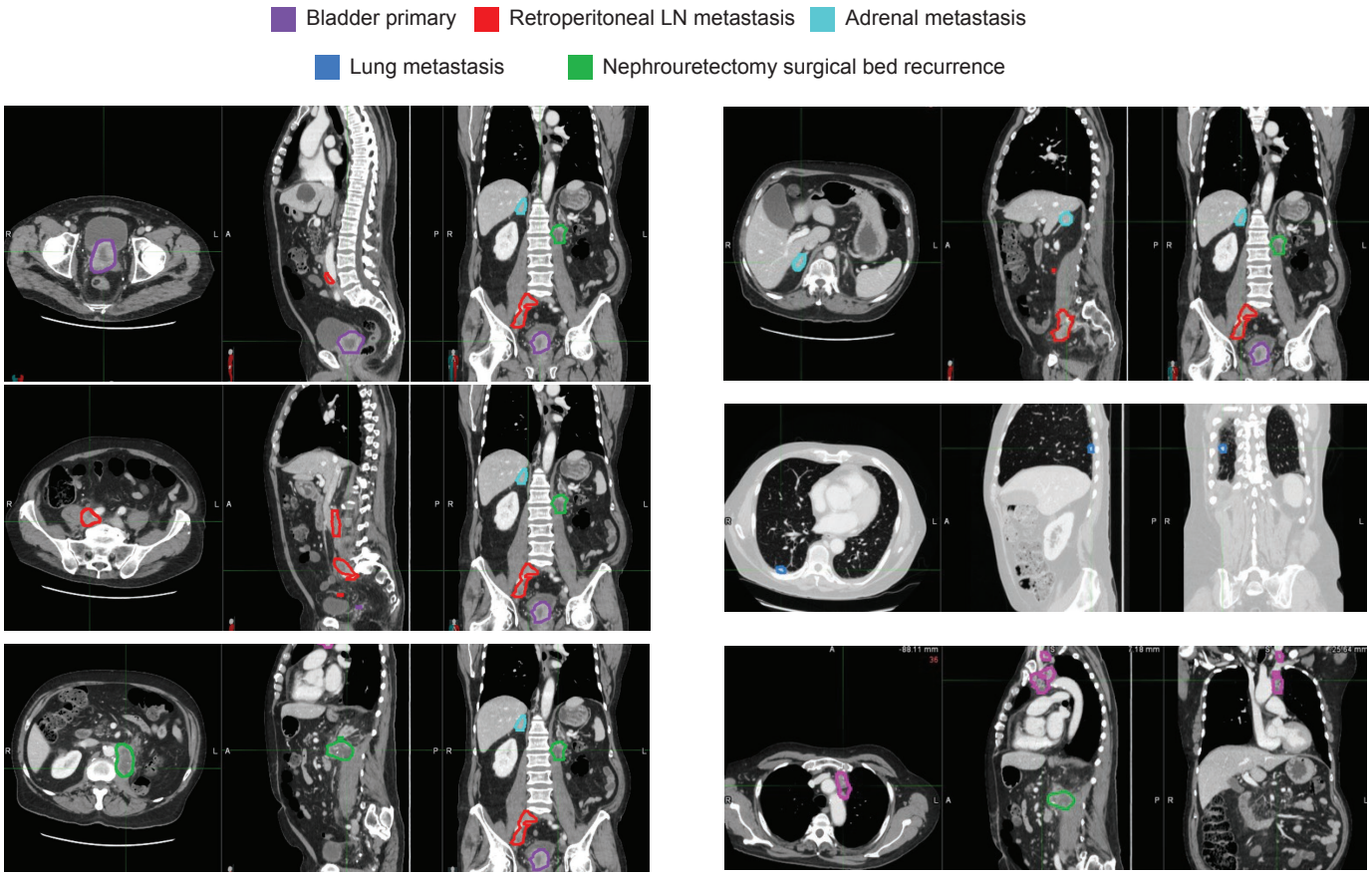

c

19-037: 4 month CT scan

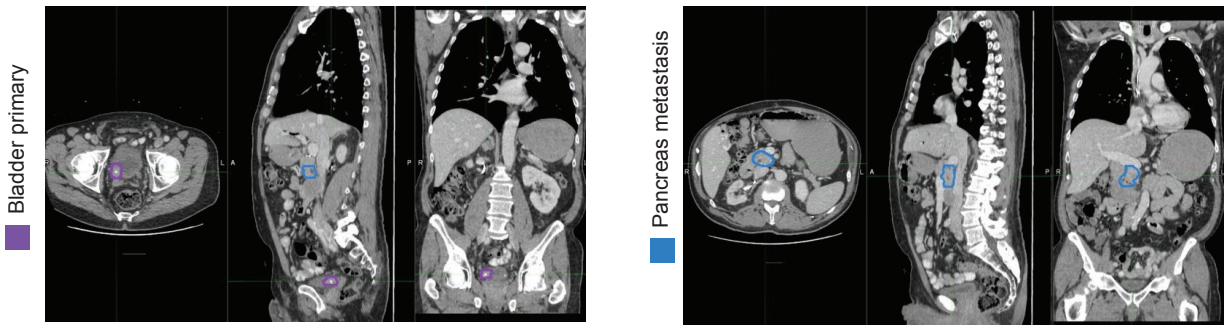

19-037: 7 month CT scan

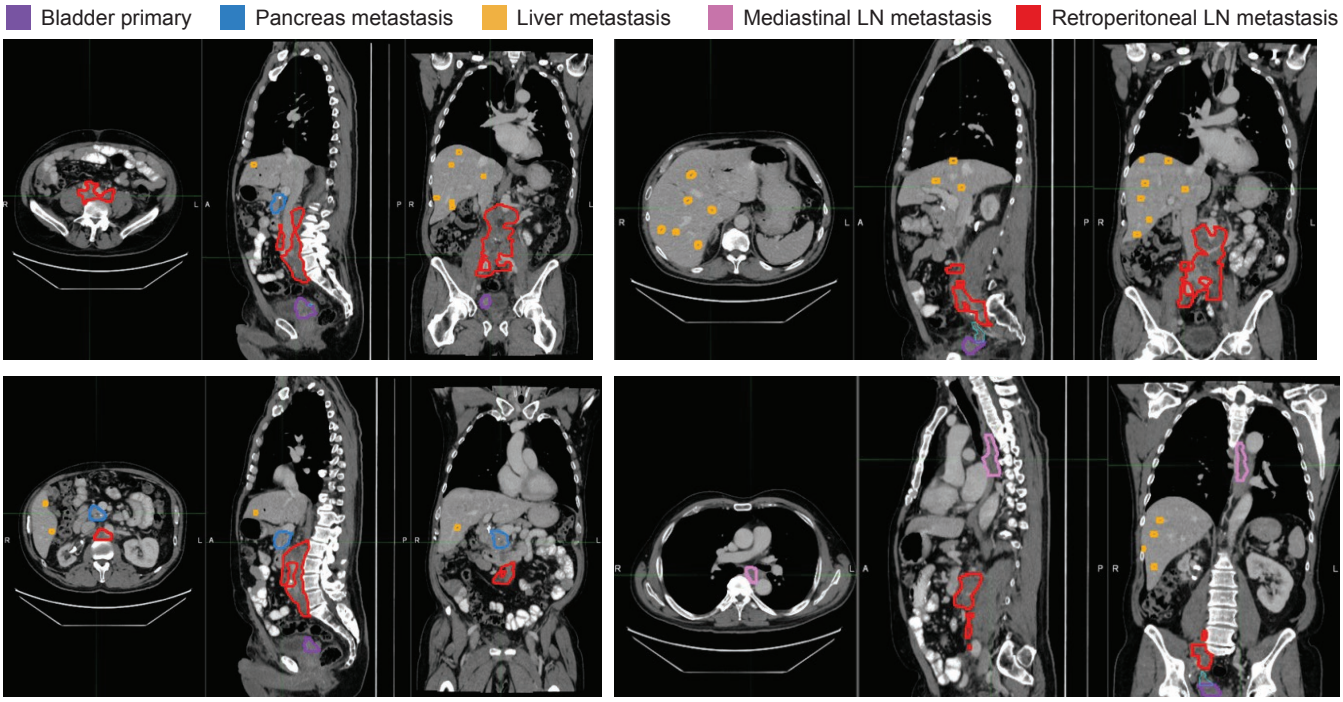

d

16-070: 3 month CT scan

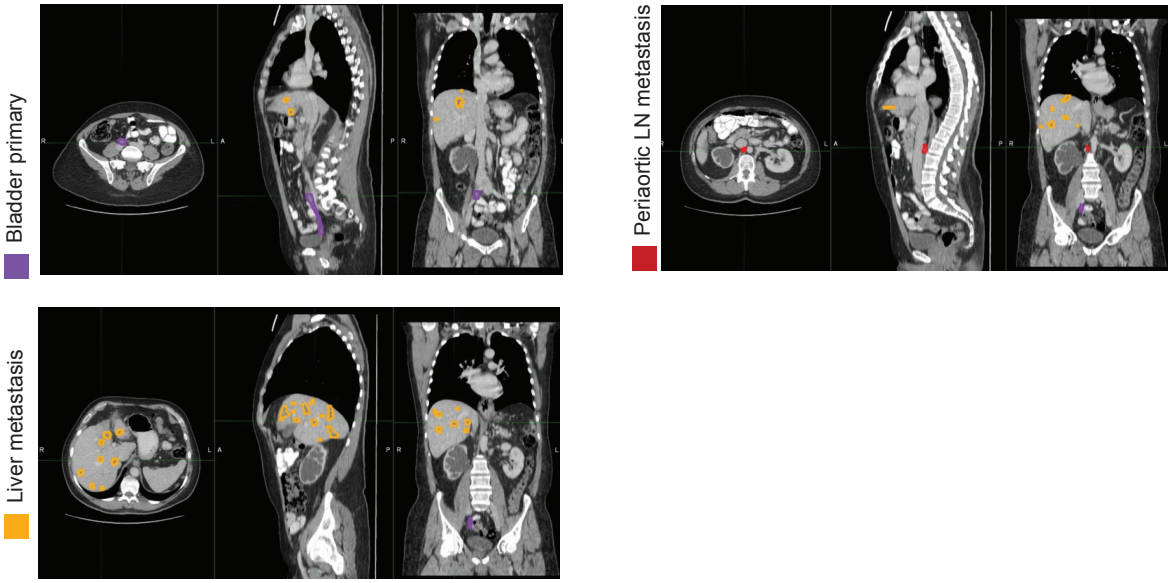

16-070: 27 month CT scan

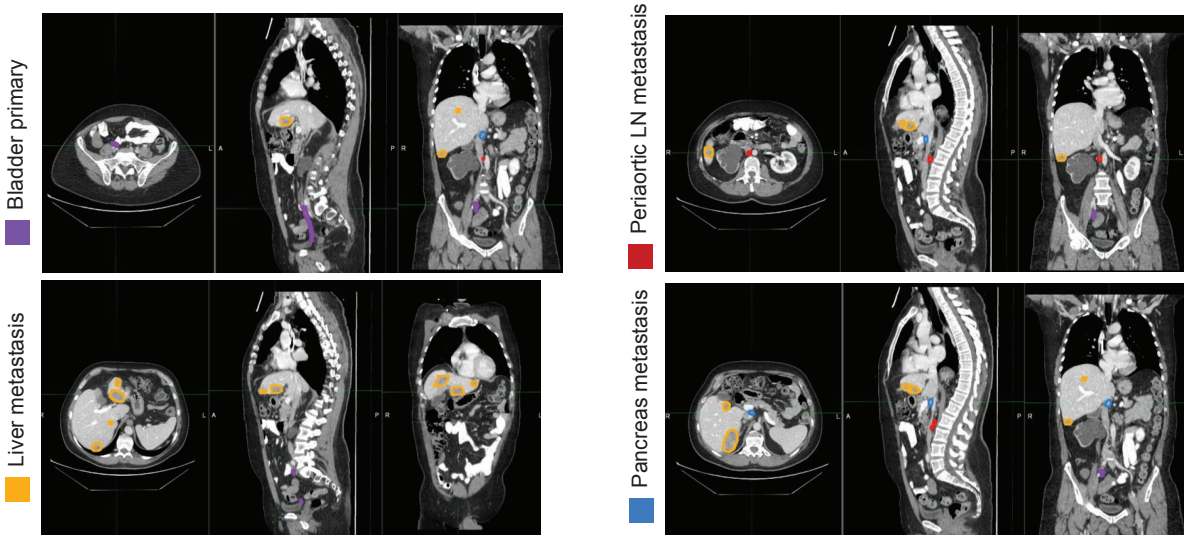

16-070: 45 month CT scan

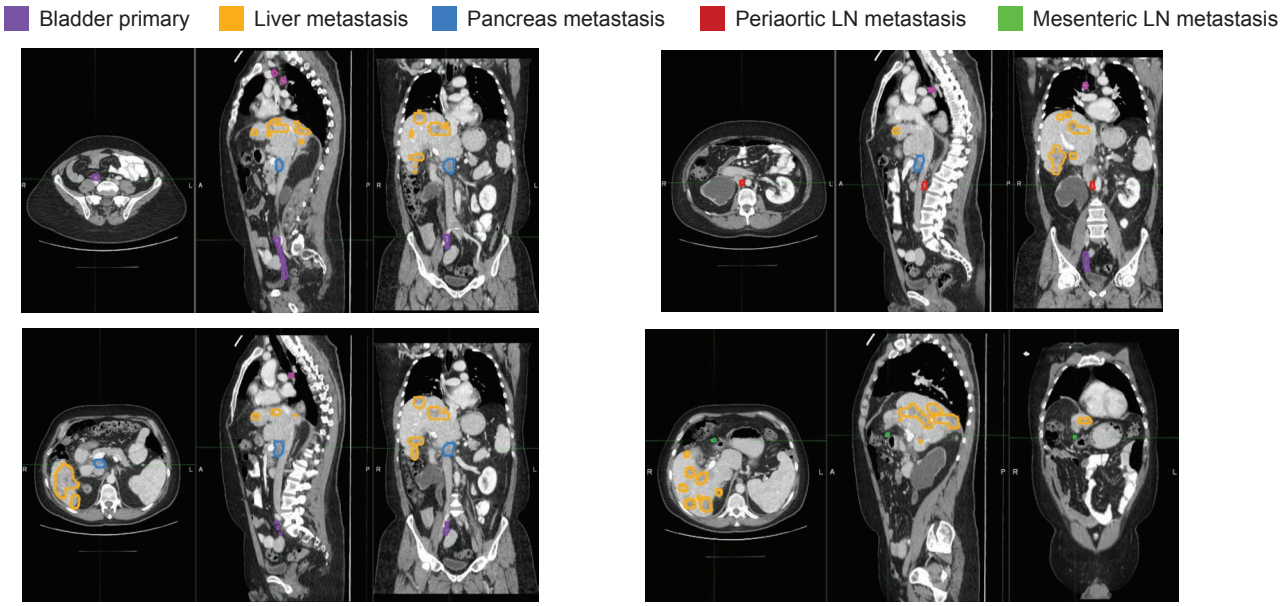

e

17-020: 2 month CT scan

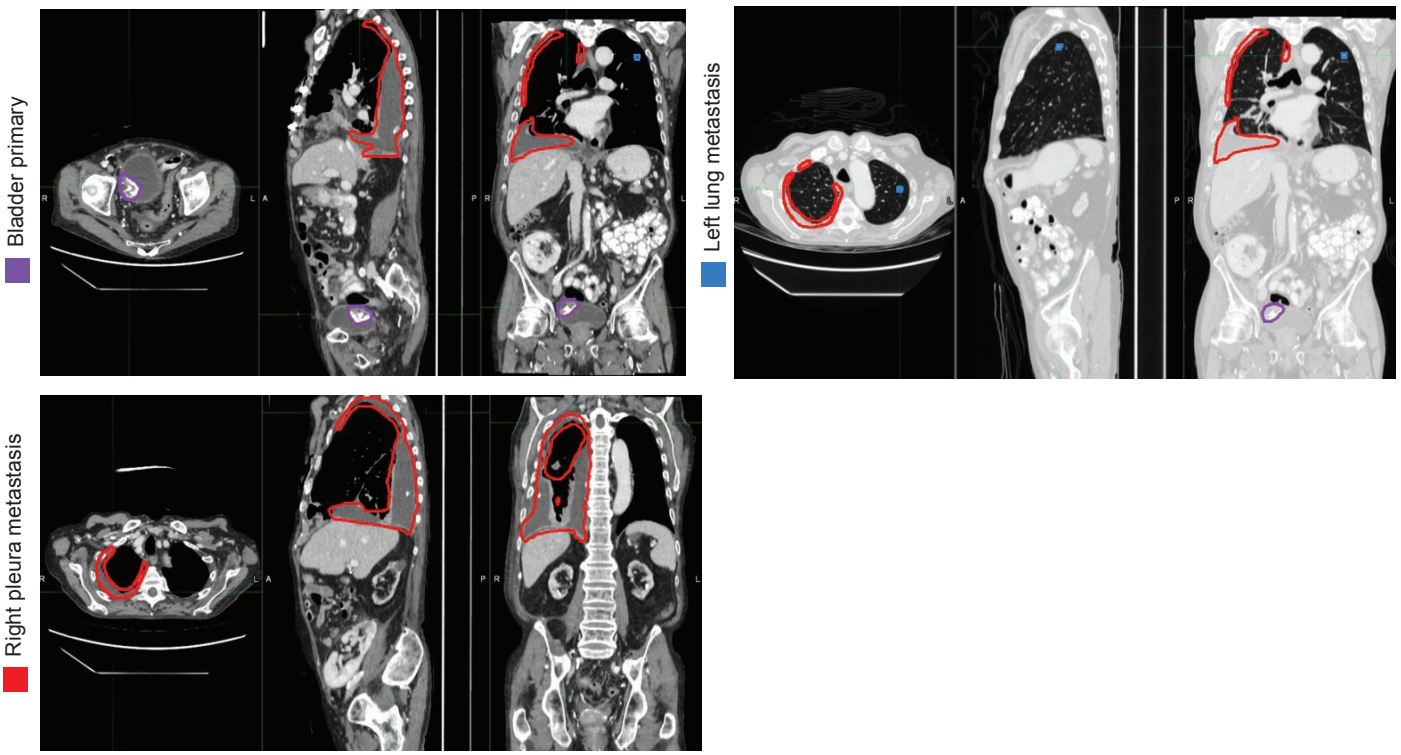

17-020: 5 month CT scan

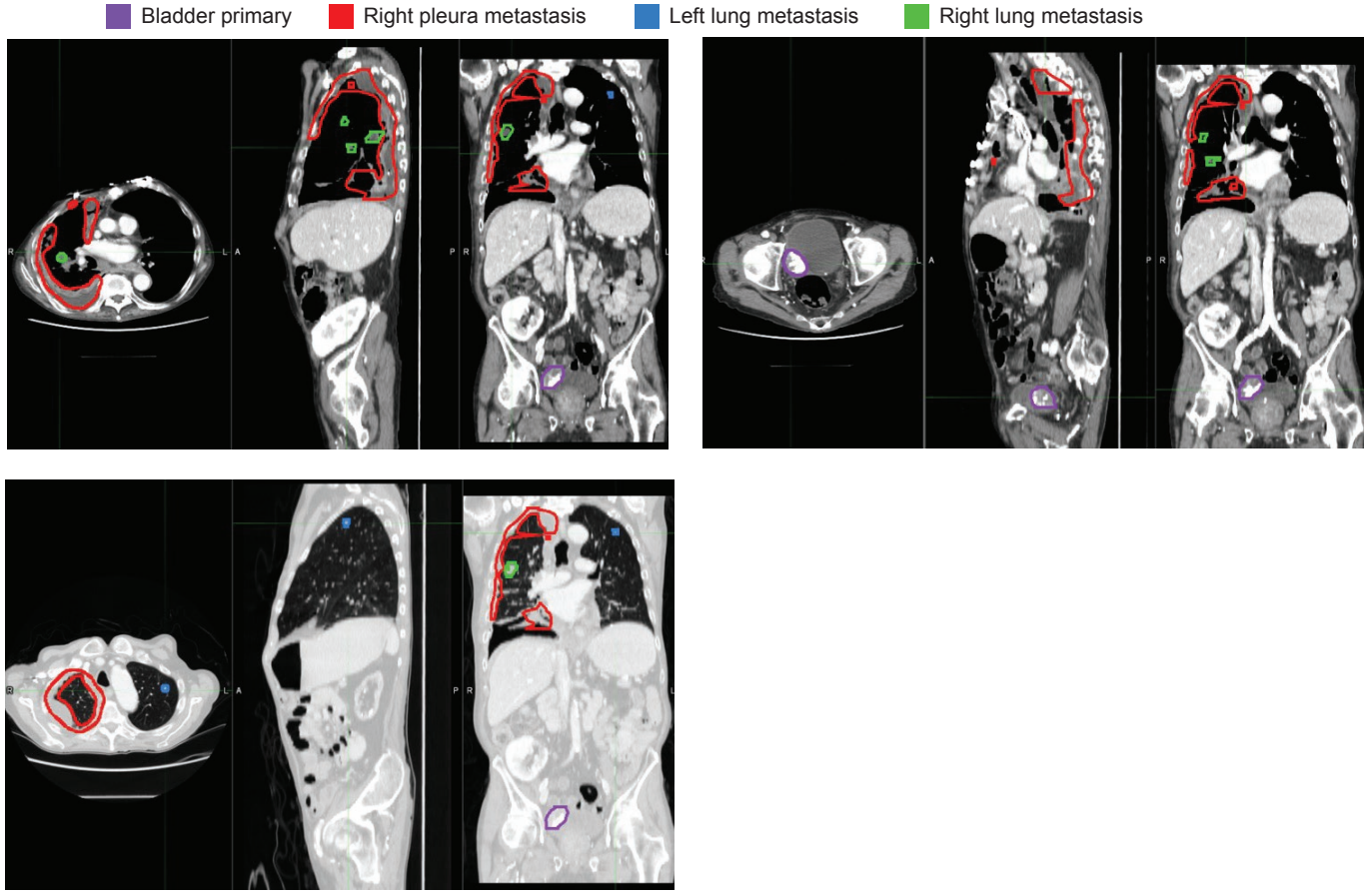

f

16-097: 3 month CT scan (10m PTD)

Liver metastasis Right lung metastasis Left lung metastasis

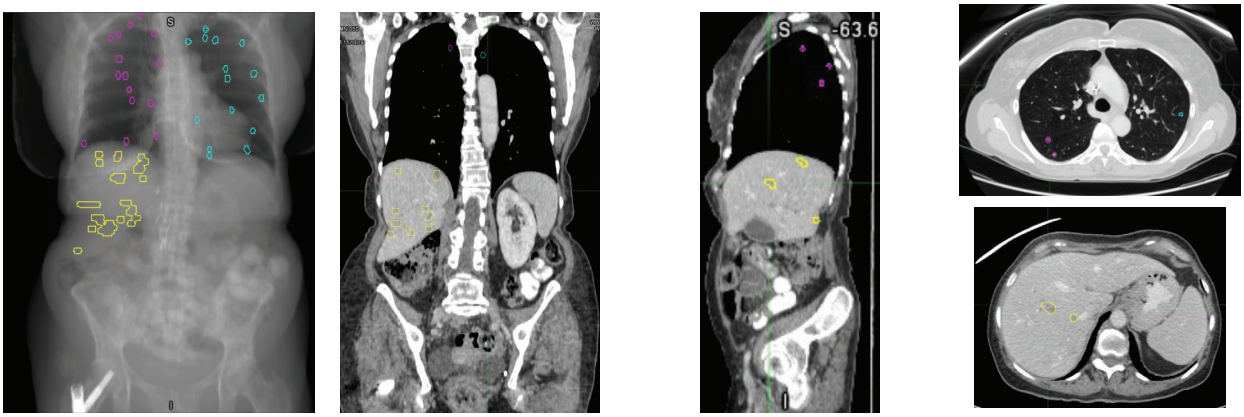

17-071: 9 month CT scan (6m PTD)

mesentery, omentum, and peri-intestinal metastases collected at autopsy were not able to be clearly matched to abdominal/peritoneal nodules visible on CT scan

Abdominal/peritoneal nodules

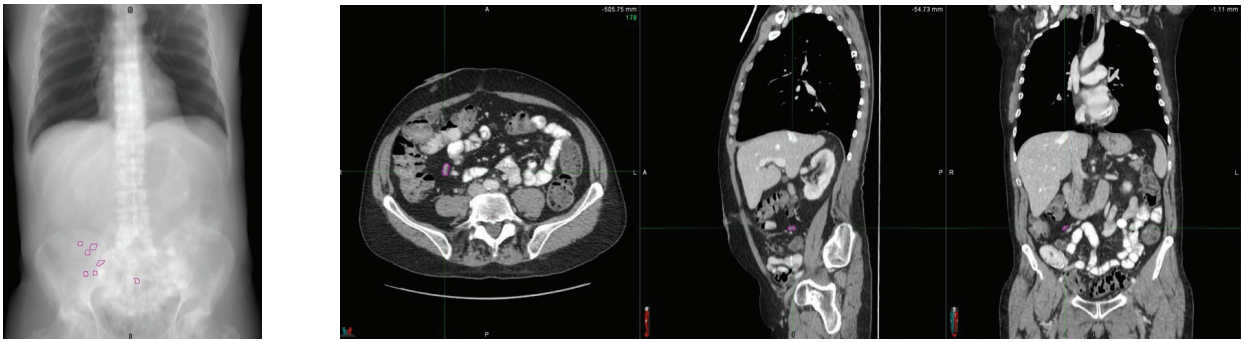

19-001: 44 month CT scan (1m PTD)

Liver metastasis Lymph node metastasis Lung metastasis

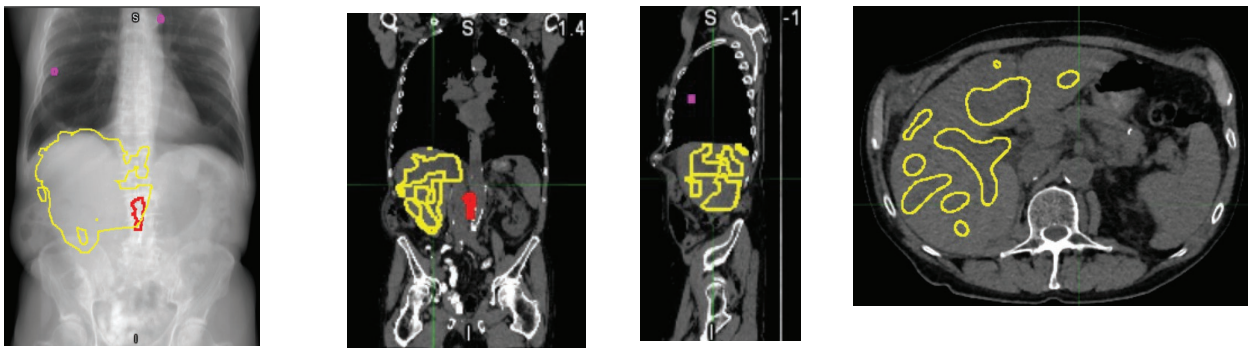

g 16-070: 23.3m PTD / 24m from Dx / 0.5m prior to ICI

Liver metastasis Periaortic LN metastasis

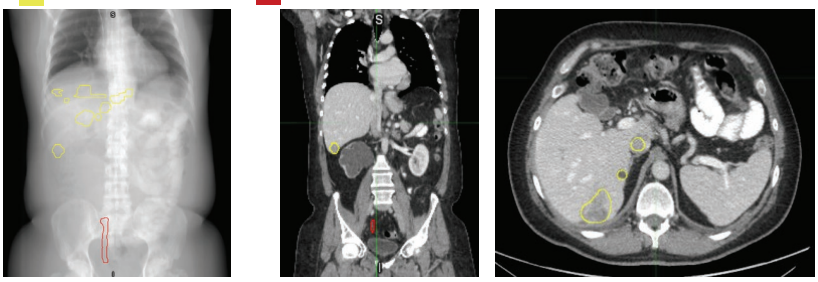

16-097: 3.1m PTD / 10m from Dx / 0.1m prior to ICI

Liver metastasis Right lung metastasis Left lung metastasis

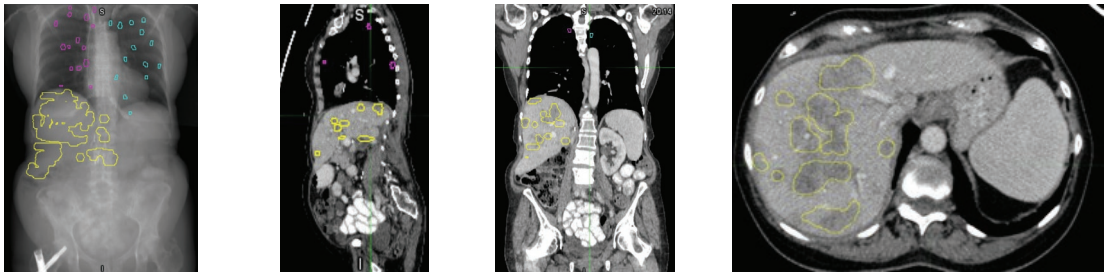

17-030: 6.1m PTD / 14m from Dx / 0.1m prior to ICI

Liver metastasis

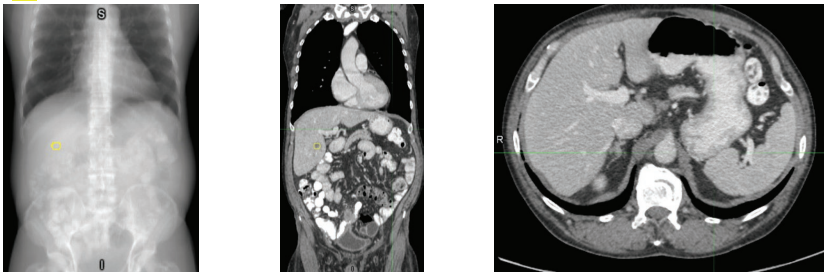

17-047: 12.2m PTD / 102m from Dx / 1.2m prior to ICI

Hilar LN metastasis Lung metastasis

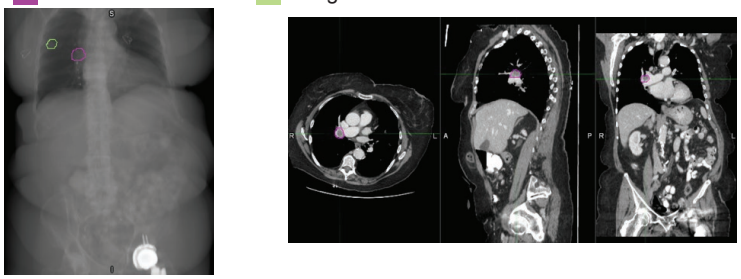

19-022: 21m PTD / 67m from Dx / 9m prior to ICI

Lung metastasis

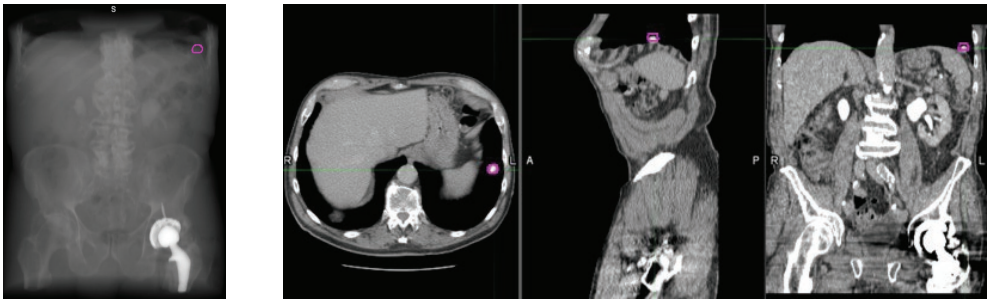

18-065: 3.4m PTD / 2m from Dx / 0.8m prior to ICI

Uterus metastasis LN metastasis

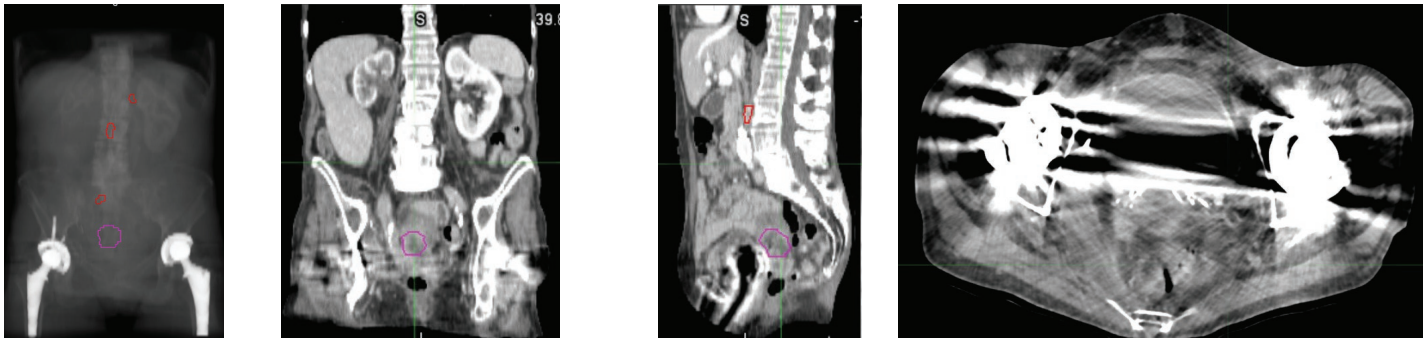

18-101: 3.2m PTD / 6m from Dx / 0.3m prior to ICI

Liver metastasis Left Kidney Peritoneum metastasis

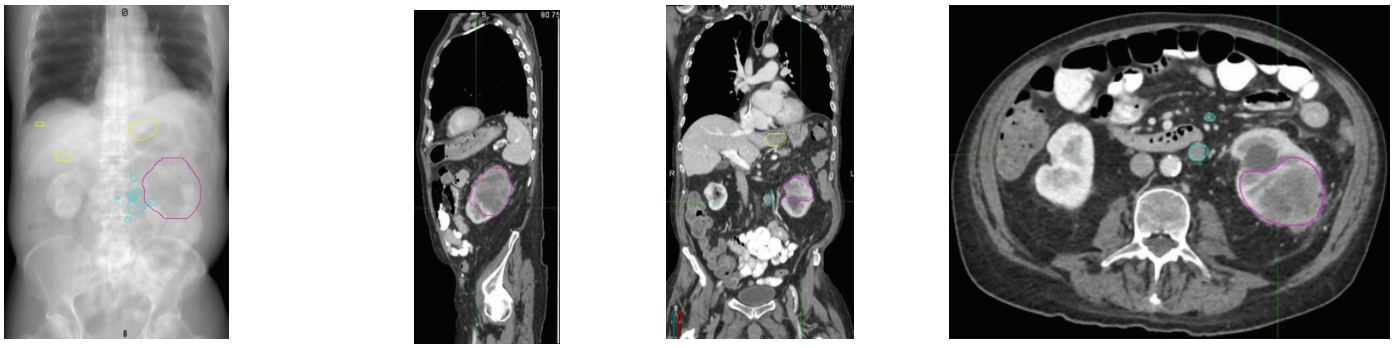

19-037: 5.3m PTD / 5m from Dx / 0.7m prior to ICI

Pancreas metastasis Bladder primary

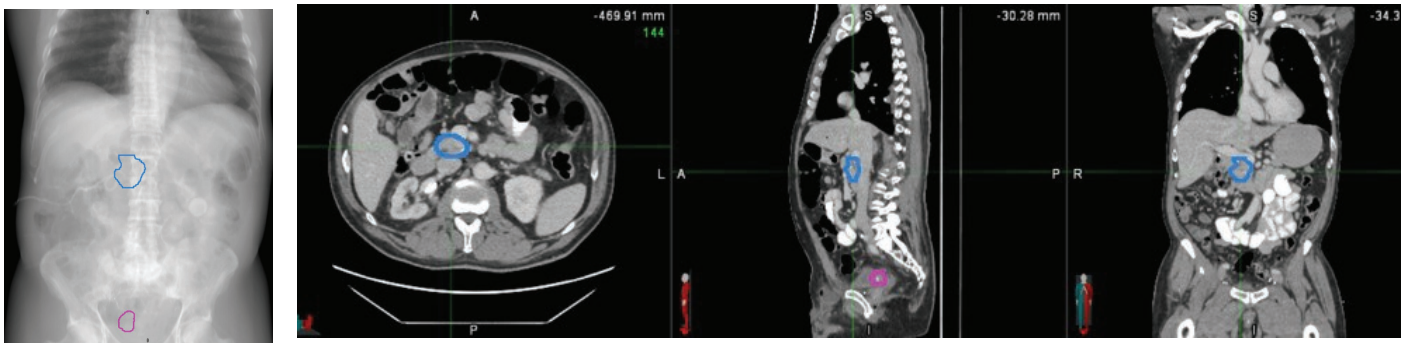

19-044: 6.8m PTD / 19m from Dx / 2.5m prior to ICI

RP LN metastasis Peri-rectal mass Pelvic wall mass

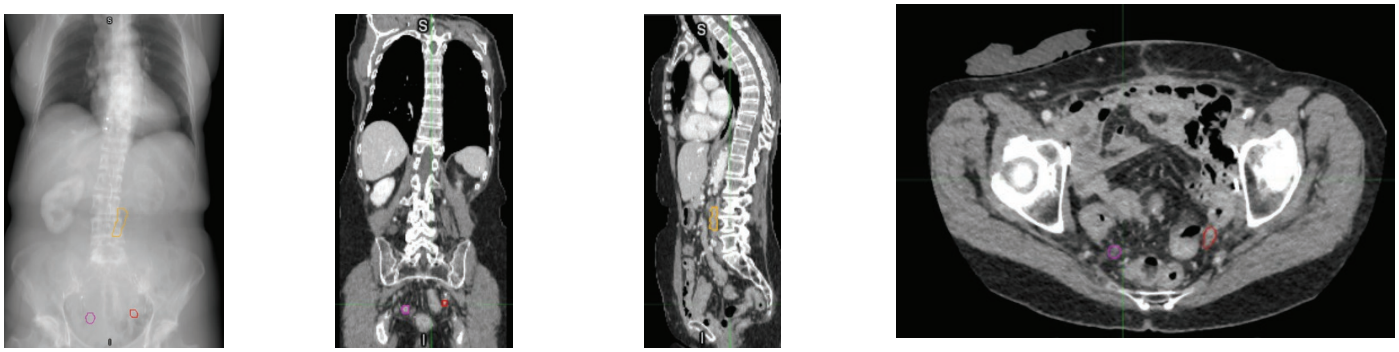

Supplementary Figure 2

a-e) Coronal, sagittal, and axial CT cross-sections from all CT scans shown in **Figure 1c** and **Extended Data Fig. 1e** as two-dimensional projections for patients 17-030 (a), 19-004 (b), 19-037 (c), 16-070 (d), and 17-020 (e). Annotated timing is months from diagnosis.

f) The first staging CT scan available for patients 16-097, 17-071, and 19-001, showing that the ordering of metastases could not be distinguished in these patients. Both two-dimensional projection images and individual coronal, sagittal, and axial CT cross-sections are shown for each. Months from diagnosis and months prior to death (PTD) annotated.

g) The staging CT scan immediately prior to start of immune checkpoint inhibitor (ICI) treatment in the nine patients 16-070, 16-097, 17-030, 17-047, 18-065, 18-101, 19-022, 19-037, 19-044 treated with at least one full cycle of ICI. Both two-dimensional projection images and individual coronal, sagittal, and axial CT cross-sections are shown for each. Months from diagnosis (Dx), prior to death (PTD) and prior to immune checkpoint inhibitor (ICI) administration annotated.

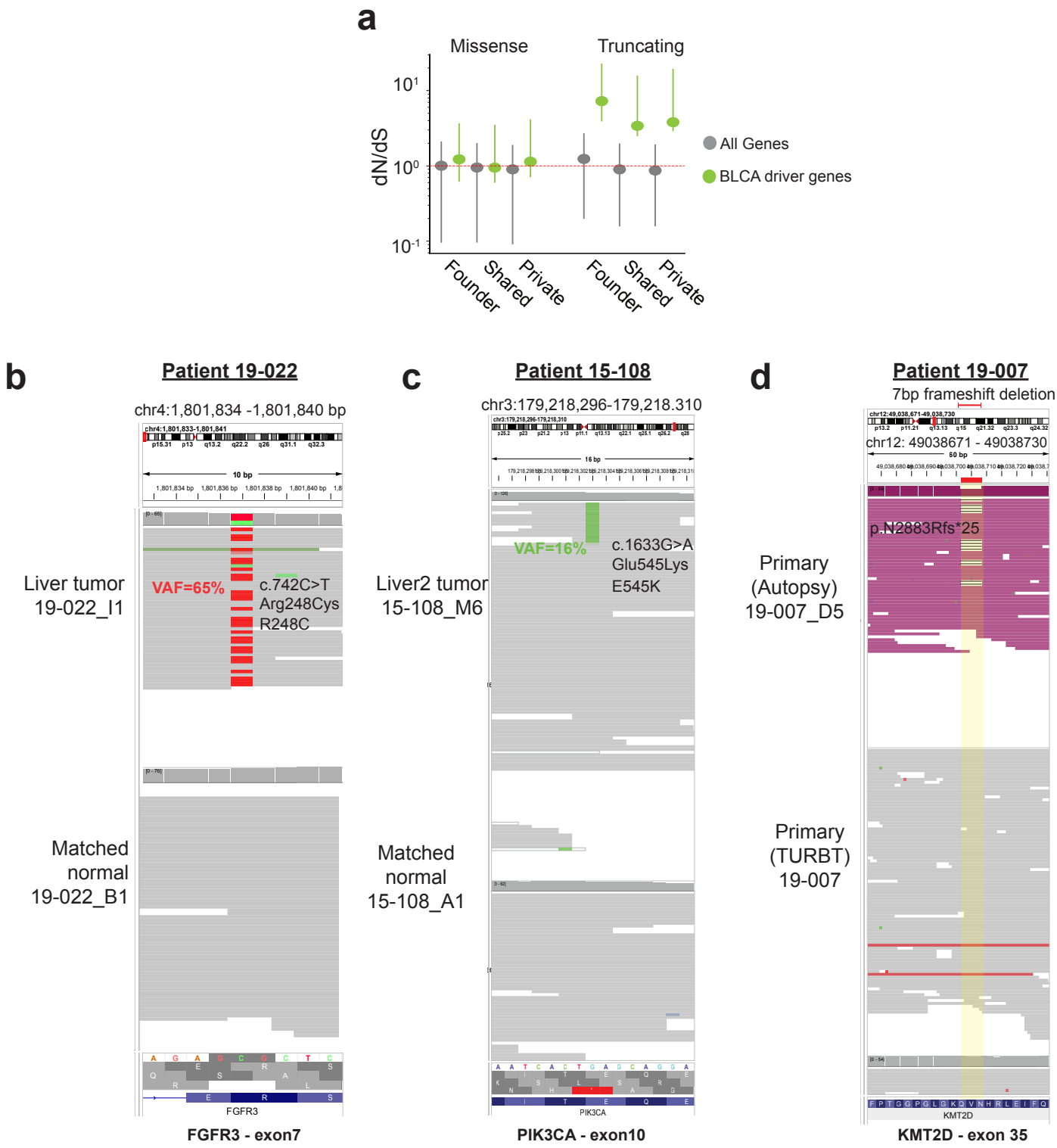

Supplementary Figure 3

a) dN/dS ratios for missense and truncating mutations across all genes or BLCA driver genes in 19 patients (excluding hypermutator patient 17-047), stratified by mutation clonality (n=19 for each clonality group). Points represent maximum likelihood estimates (MLEs); error bars indicate 95% confidence intervals.

b) IGV screenshot showing presence of private mutation in *FGFR3* in patient 19-022 Liver metastasis and absent in matched normal.

c) IGV screenshot showing presence of private mutation in *PIK3CA* in patient 15-108 Liver metastasis and absent in matched normal.

d) IGV screenshot showing presence of private deletion in *KMT2D* in patient 19-007 primary collected at autopsy and absent in primary at TURBT.

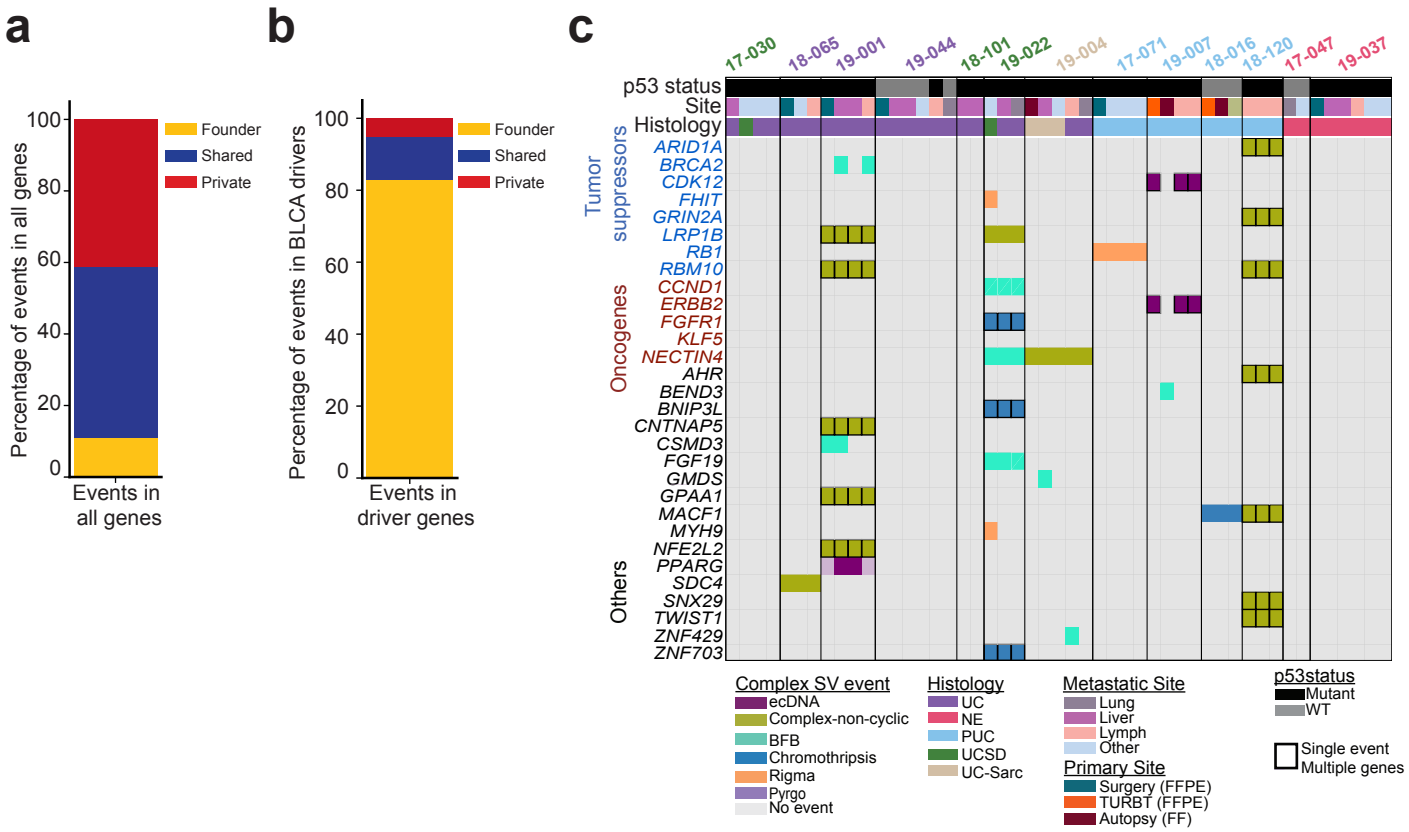

Supplementary Figure 4

a) Percentage of genome-wide complex SVs with founder, shared, and private status as detected by JaBbA and Amplicon Architect (see Methods).

b) Percentage of complex SV events that include BLCA driver genes that are founder, shared, and private (status assigned through manual curation).

c) Comut plot of driver genes involved in complex SV events. Multiple genes involved in the same amplicon or footprint are indicated by black boxes. Sample level histology and p53 mutation status (presence of a mutation in exonic region) are also denoted.

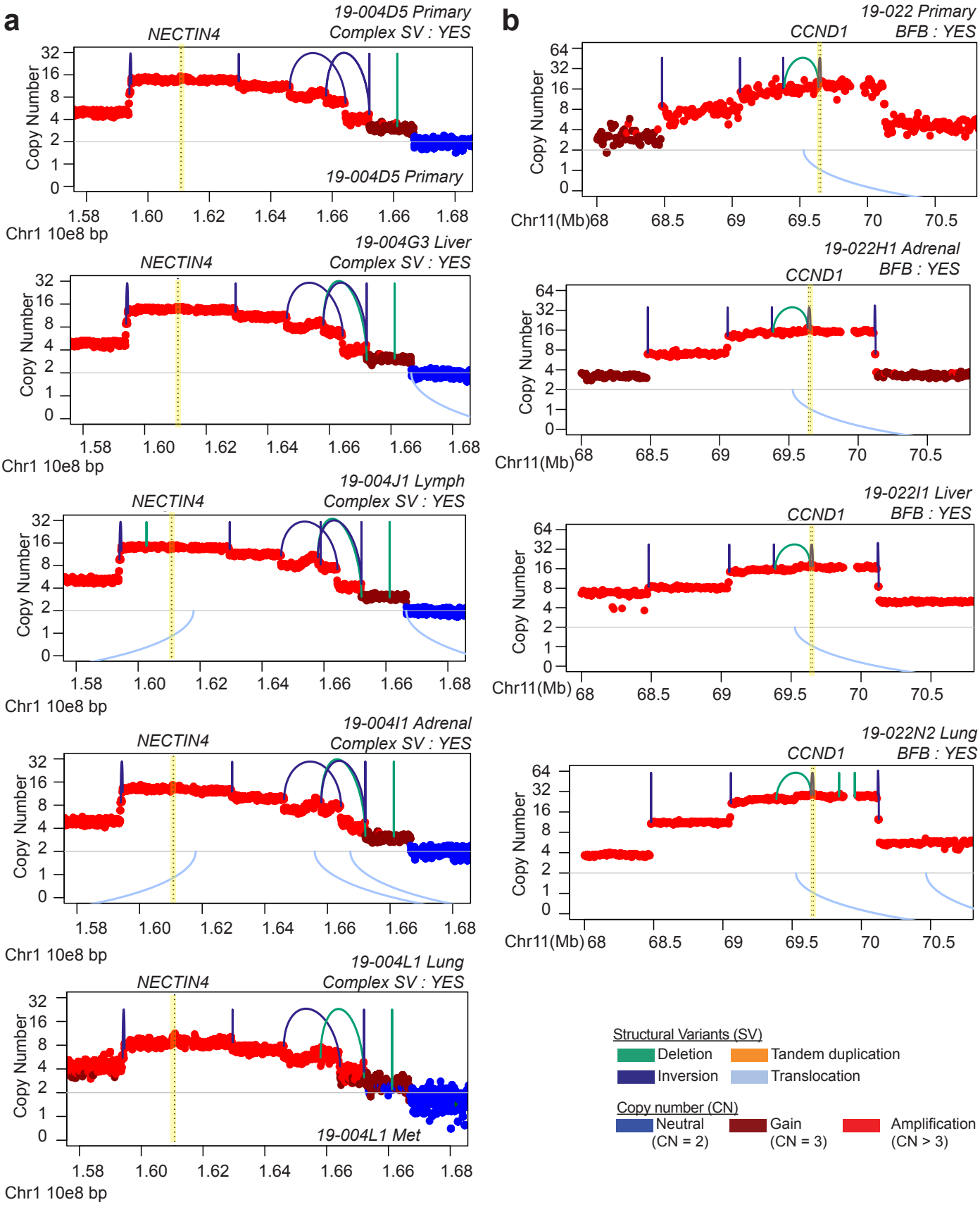

Supplementary Figure 5

a) Complex SV involving *NECTIN4* in patent 19-004 highlighting the early evolution (Founder event) across primary and all metastases.

b) Breakage fusion bridge (BFB) involving *CCND1* in 19-022 highlighting the early evolution (Founder event) across primary and all metastases.

Patient 19-007 - Autopsy Primary

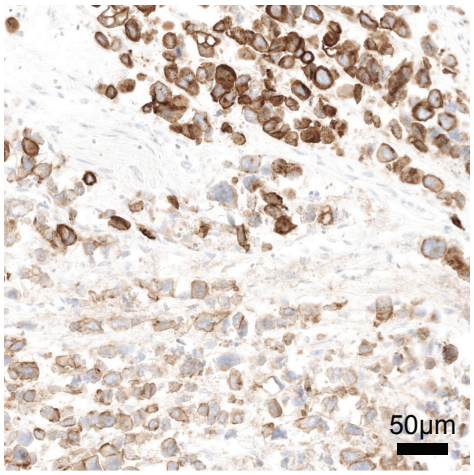

HER2 (-): 2%
HER2 (+): 19%
HER2 (++): 18%
HER2 (+++): 60%

Patient 19-007 (H1) - Metastasis
Retroperitoneal lymph node

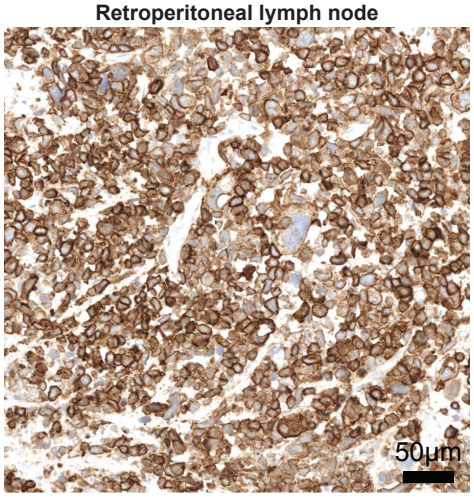

HER2 (-): 0%
HER2 (+): 1.6%
HER2 (++): 12%
HER2 (+++): 87%

Patient 19-007 (K1) - Metastasis
Iliac lymph node

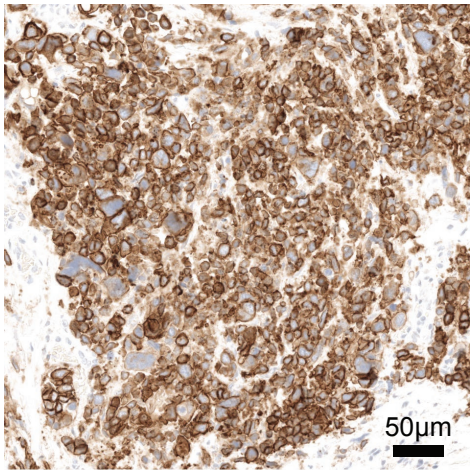

HER2 (-): 0.3%
HER2 (+): 1%
HER2 (++): 18%
HER2 (+++): 80%

Supplementary Figure 6

Additional representative images from 19-007 primary and lymph node metastases stained for HER2 protein. Percentage of cells at each HER2 staining intensity shown at right. IHC staining was performed on a single patient Tissue Microarray (TMA). For each tumor, three cores were assessed for HER2 staining intensity and reproduced similar results.

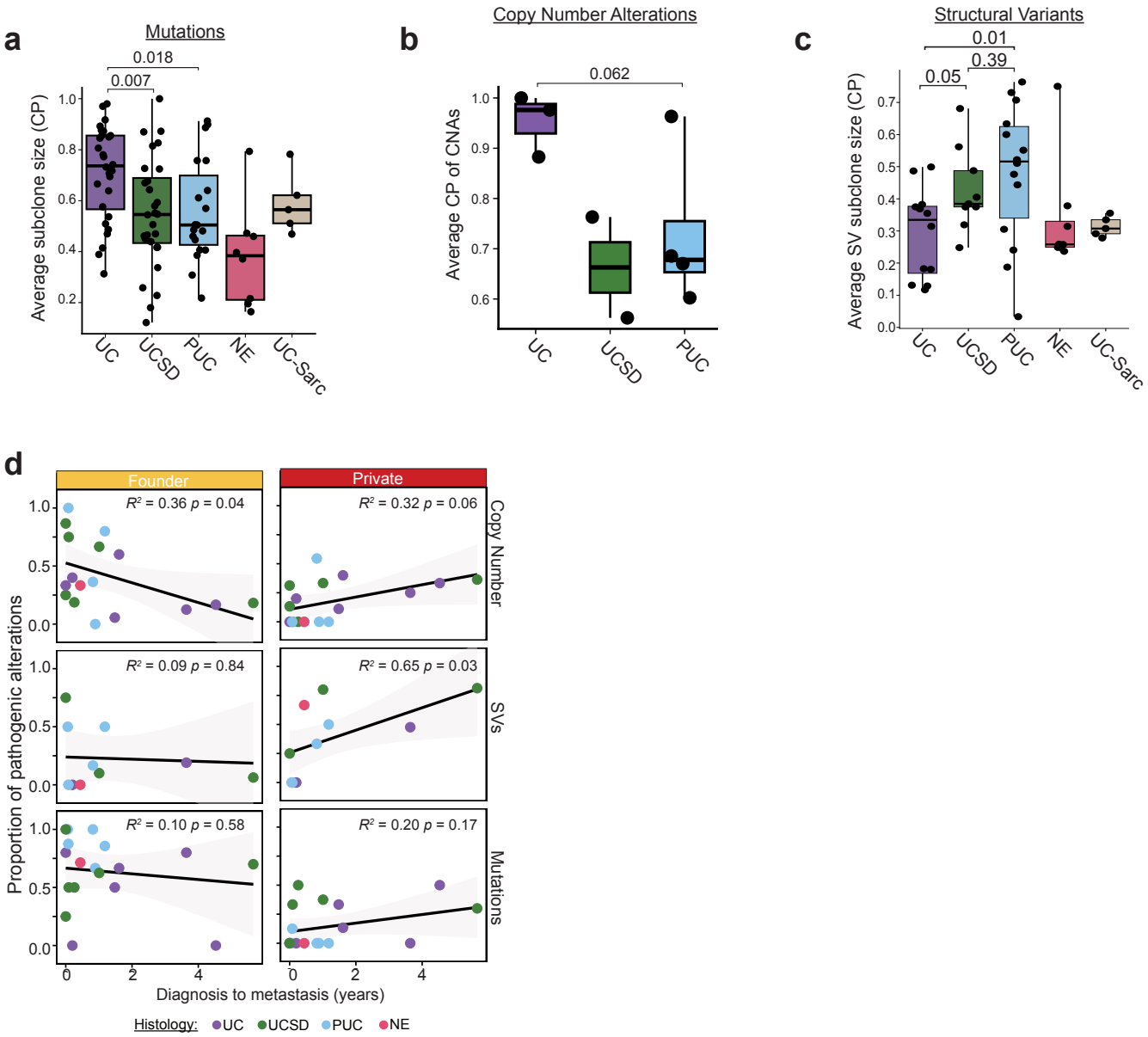

Supplementary Figure 7

a) Average clonality of mutations in each tumor, calculated as mean cellular prevalence (CP) of the shared and private mutation clones (clones with CP > 0.03 and mutations with alternate reads >4) present in that tumor (UC, n=28; UCSD, n=28; PUC, n=19; NE, n=8; UC-Sarc, n=5). P-values from unadjusted two-sided Mann-Whitney U-tests.

b) Average clonality of CNAs in each patient, calculated from snRNA-seq Numbat analysis as the mean cellular prevalence (CP) of all CNAs (UC, n=3; UCSD, n=2; PUC, n=4). P-values from unadjusted two-sided Mann-Whitney U-tests.

c) Average clonality of SVs in each tumor from 13 patients with WGS, calculated using k-means clustering of SVclone-derived CCF profiles (UC, n=12; UCSD, n=9; PUC, n=14; NE, n=8; UC-Sarc, n=5). SVs were clustered based on similarity in CCF across samples, and cluster means represent the average clonality of co-clustered variants. P-values from unadjusted two-sided Mann-Whitney U-tests.

d) Proportion of founder or private pathogenic alterations in each patient in relation to the time from diagnosis to metastasis (years). Unadjusted p-values from two-sided Wald test of a linear model with number of tumors per patient, total number of treatments, and percentage mean UC per patient as co-variates. Shaded areas indicate 95% confidence interval around the regression line.

Boxplots show median bounded by interquartile ranges (IQR), whiskers to 1.5× IQR.

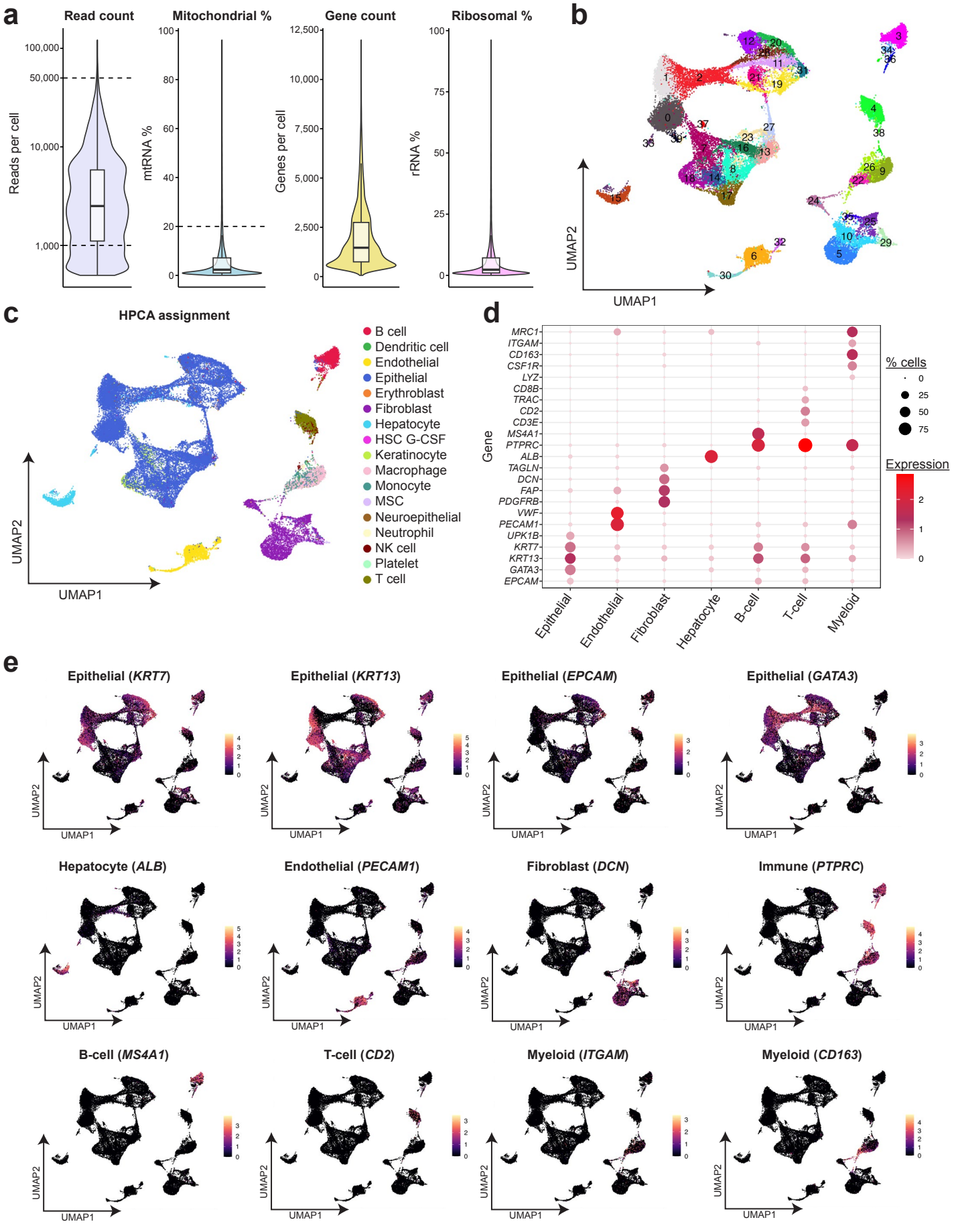
a
Read count
Mitochondrial %
Gene count
Ribosomal %
Reads per cell
mtRNA %
Genes per cell
rRNA %
b
UMAP2
UMAP1
c
HPCA assignment
B cell
Dendritic cell
Endothelial
Epithelial
Erythroblast
Fibroblast
Hepatocyte
HSC G-CSF
Keratinocyte
Macrophage
Monocyte
MSC
Neuroepithelial
Neutrophil
NK cell
Platelet
T cell
d
Gene
% cells
Expression
Epithelial
Endothelial
Fibroblast
Hepatocyte
B-cell
T-cell
Myeloid
e
Epithelial (KRT7)
Epithelial (KRT13)
Epithelial (EPCAM)
Epithelial (GATA3)
Hepatocyte (ALB)
Endothelial (PECAM1)
Fibroblast (DCN)
Immune (PTPRC)
B-cell (MS4A1)
T-cell (CD2)
Myeloid (ITGAM)
Myeloid (CD163)

Supplementary Figure 8

a) Quality control metrics and filtering for snRNA-seq dataset across 9 patients and 15 tumors. Plots display the distribution of all unfiltered cells (n = 59,279) across QC metrics, with dashed lines indicating filters applied to the finalized dataset. Boxplots show median bounded by interquartile ranges (IQR), whiskers to 1.5× IQR.

b-c) UMAP of all snRNA-seq cells passing quality filters, colored by (b) Louvain cluster or (c) assignment of each cell to the Human Primary Cell Atlas cell types.

d) Cell type marker expression in each curated cell type. Color indicates average expression across all cells of that cell type and size indicates proportion of cell type with expression above zero.

e) UMAPs of all snRNA-seq cells passing quality filters, colored by cell type marker expression.